Applied Research Laboratory

Technical Report

BOTTOM CONTOUR INFLUENCE ON RAY TRACING
by

Shaari M. Unger

PENNSTATE

The Pennsylvania State University
APPLIED RESEARCH LABORATORY
P.O. Box 30
State College, PA 16804

BOTTOM CONTOUR INFLUENCE ON RAY TRACING

by

Shaari M. Unger

Technical Report No. TR 91-011
October 1991

Supported by:
Naval Undersea Warfare Engineering Station

L.R. Hettche, Director
Applied Research Laboratory

Unclassified

SECURITY CLASSIFICATION OF THIS PAGE

REPORT DOCUMENTATION PAGE

1a REPORT SECURITY CLASSIFICATION UnClassified	1b. RESTRICTIVE MARKINGS
2a SECURITY CLASSIFICATION AUTHORITY Unclassified	3 DISTRIBUTION / AVAILABILITY OF REPORT
2b DECLASSIFICATION / DOWNGRADING SCHEDULE	
4 PERFORMING ORGANIZATION REPORT NUMBER(S)	5 MONITORING ORGANIZATION REPORT NUMBER(S) TR# 91-011
6a NAME OF PERFORMING ORGANIZATION Applied Research Laboratory 6b OFFICE SYMBOL (If applicable) ARL	7a. NAME OF MONITORING ORGANIZATION
6c ADDRESS (City, State, and ZIP Code) P.O. Box 30 State College, PA 16804	7b. ADDRESS (City, State, and ZIP Code)
8a NAME OF FUNDING / SPONSORING ORGANIZATION NUWES 8b OFFICE SYMBOL (If applicable) ARL	9 PROCUREMENT INSTRUMENT IDENTIFICATION NUMBER
8c ADDRESS (City, State, and ZIP Code) Naval Undersea Warfare Engineering Station Keyport, Washington 98345-0580	10 SOURCE OF FUNDING NUMBERS PROGRAM ELEMENT NO / PROJECT NO / TASK NO. / WORK UNIT ACCESSION NO
11 TITLE (Include Security Classification) Bottom Contour Influence on Ray Tracing	
12 PERSONAL AUTHOR(S) Shaari Michal Unger	
13a TYPE OF REPORT 13b TIME COVERED FROM _____ TO _____ 14 DATE OF REPORT (Year, Month, Day) August 1991 15 PAGE COUNT 32	
16 SUPPLEMENTARY NOTATION	

17 COSATI CODES			18 SUBJECT TERMS (Continue on reverse if necessary and identify by block number)
FIELD	GROUP	SUB-GROUP	bottom contour, ray tracing, HARPO, attenuation, path length, angle of incidence, in-situ

19 ABSTRACT (Continue on reverse if necessary and identify by block number)

Previously used ray trace models have assumed flat bottom boundary conditions. This qualitative study shows the impact of modeling bottom contour irregularities on the predictability of sound rays and thus on transmission loss. The HARPO ray trace model is presented, and qualitative results are examined between several bottom contour variations. The effects of changes in bottom contour were assessed. THese irregularities caused changes in attenuation, path length and angles of incidence.

The results of a study which measured in-situ data from three equally spaced receivers are also discussed. Acoustic receive levels were comparable. Test suggestions are proposed for obtaining quantitative transmission loss values.

20 DISTRIBUTION / AVAILABILITY OF ABSTRACT ☐ UNCLASSIFIED/UNLIMITED ☐ SAME AS RPT ☐ DTIC USERS	21 ABSTRACT SECURITY CLASSIFICATION
22a NAME OF RESPONSIBLE INDIVIDUAL	22b TELEPHONE (Include Area Code) / 22c. OFFICE SYMBOL

DD FORM 1473, 84 MAR 83 APR edition may be used until exhausted
All other editions are obsolete

SECURITY CLASSIFICATION OF THIS PAGE

Unclassified

Abstract

Previously used ray trace models have assumed flat bottom boundary conditions. This qualitative study shows the impact of modeling bottom contour irregularities on the predictability of sound rays and thus on transmission loss. The HARPO ray trace model is presented, and qualitative results are examined between several bottom contour variations. The effects of changes in bottom contour were assessed. These irregularities caused changes in attenuation, path length and angles of incidence.

The results of a study which measured in-situ data from three equally spaced receivers are also discussed. Acoustic receive levels were comparable. Test suggestions are proposed for obtaining quantitative transmission loss values.

TABLE OF CONTENTS

LIST OF FIGURES

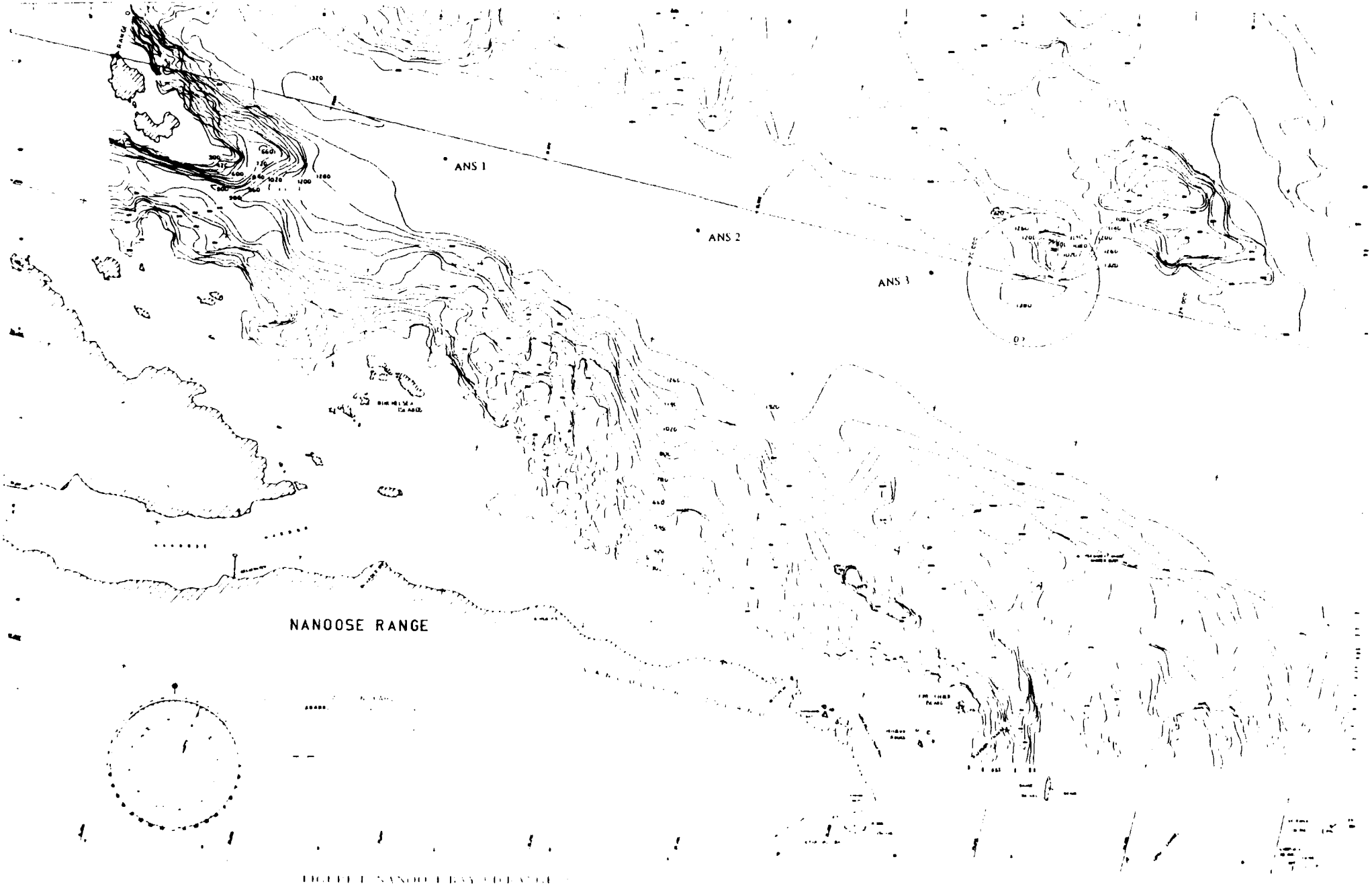
ANS 1
ANS 2
ANS 3
NANOOSE RANGE

CHAPTER 1

PROBLEM DEFINITION

1.1 INTRODUCTION

The objective of this paper is to qualitatively determine the effect changes in bottom contour will have on sound propagation using ray trace techniques. This study will describe some bathymetric properties of the Nanoose Bay range. It will outline the Hamiltonian Acoustic Ray Tracing Program for the Ocean (HARPO), a ray theory based model, and discuss the relationship between ray tracing and transmission loss. HARPO ray traces will be used to portray the changes in the propagation of sound as changes in bottom contour are introduced. In-situ measurements acquired from three receivers over a relatively flat contour are also examined.

Staal and Desharnais [1] used a propagation loss model, (PROLOS), developed by Defense Research Establishment Atlantic (DREA), Dartmouth (Nova Scotia) in relation with in-situ measurements in Nova Scotia, over both a smooth and rough seabed. PROLOS is a range-dependent normal-mode program. There are many other propagation models available that are not range dependent, nor do they address the bottom contour, some of these are listed in Appendix A.

The Naval Undersea Warfare Engineering Station (NUWES) uses the Nanoose Bay test range, and others like it, to verify weapon radiated noise and test weapon tactics. It is important to know about the acoustic properties of Nanoose Bay and how the terrain will influence sound propagation. NUWES currently models its instrumented test sites assuming a flat bottom contour. With newly available ray trace models, it is prudent to reevaluate some old and trusted ray tracing methods and to incorporate some contour into the current ray trace model for known areas to better predict sound propagation. NUWES analysts are concerned with

measurement accuracy and water conditions in relation to transmission loss over short ranges for evaluating vehicle radiated noise. During radiated noise data acquisition, hydrophone saturation or inadequate signal to noise could contaminate radiated data. Acoustic analysis techniques, described by Keys [2], are also used to assess vehicle and machinery performance by correlating vibration data to radiated noise characteristics.

During vehicle tests on range a directional source may be aimed towards a steep slope or hill. The change from flat to sloped bottom contour changes the grazing angle which results in an altered reflection coefficient. Reflection coefficient changes cause differences in ray angles, and thus move focal point locations. Active sonar systems can be attracted to these focal locations. Change in the sound propagation path causes increased signal-to-noise, reverberation and focusing effects. High frequency sound is strongly affected by boundary scattering and microstructure variability, but low frequency sound is most affected by sea floor properties. This will be discussed in detail in the following chapters.

1.2 DESCRIPTION OF NANOOSE RANGE

The Nanoose range site, shown in Figure 1 [3], is an instrumented underwater tracking range used to measure radiated noise and evaluate active and passive acoustic systems. The unique silhouette of the area is well suited for use as an example to evaluate the influence of bottom contour on sound propagation. It is situated on the western half of the Strait of Georgia, offshore of Nanoose Bay and Ballenas Channel, and approximately 18 kilometers (km) north of Nanaimo, B.C., Canada. The maximum dimensions of the range are 25.5 km (east-west) by 12.4 km (north-south). It includes the north end of a deep trough within the Strait of Georgia, which extends from the Ballenas Islands in the northwestern portion of the range in an east by southeast direction to central portions of the Strait located between Sand

Head on the Fraser River Estuary and Valdes Island. The sides of the basin are irregular with occasional outcroppings. The lower slopes (200 - 400 meters deep) have more than 10 meters of mud. Bottom samples show 40-70% clay, 5% sand (diameter 0.625mm-2mm), and diatomacious ooze and mud make up the rest. The average porosity is 75%. Middleton [4], and Herlinveaux Garrison [5] discuss the bathymetry, geography and climatology of the Nanoose range in more detail. The Nanoose Bay test range was selected for this study because of its steep sides and irregular terrain. NUWES currently uses this range daily for measuring radiated noise from anti-submarine warfare weapons. The transmission loss equations currently used by NUWES do not take this terrain into account, and thus may be in error.

The main loss mechanisms are volume absorption, geometrical spreading loss (spherical, cylindrical *etc.*), bottom reflection loss and surface and bottom scattering loss. Volume absorption in sea water is caused by viscous effects and chemical relaxation, which increase with increasing frequency [6]. The bottom is acoustically absorptive compared to the surface (this is often referred to as a "lossy" bottom). There are some acoustic problems where knowledge of sound propagation as it is affected by bottom contour would be useful.

1.3 RAY THEORY AND TRANSMISSION LOSS

The Eikonal equation (1) is the basis of ray theory. First, assume an approximate solution to the wave equation in terms of an asymptotic series. Next substitute the asymptotic series into the wave equation. This leads to

$$|\Delta W|^2 = n^2 = c_o^2/c(R,Z_i)^2 \qquad (1)$$

where

ΔW is the gradient measured in meters

n is the index of refraction

c_0 is the initial speed of sound

$c(R,Z_i)$ is the speed of sound at range, R and depth Z_i

which determines the ray paths, and energy transportation. The change in phase is directly proportional to sound speed [7] and it is not a function of time or frequency. Along the ray path, loss varies with geometric spreading.

Limit the Eikonal equation for the case of the ray path in the vertical gradient where the water is horizontally stratified. If there is an upward slope, the shortened depth would interact with the rays causing increased bottom loss and steeper ray angles. If the projector is located at a depth, Z_i where $c(Z_i) = c_0$, n is the refractive index and θ_0 is the direction of the ray at this point, then

$$\cos\theta / \cos\theta_0 = c/c_0 = 1/n \qquad (2)$$

which is Snell's Law.

Ray theory can be used to solve the Helmholtz equation. In ray theory, waves travel along trajectories called rays. The wave speed is determined by the medium's refractive index. Rays bend in response to gradients in the refractive index. A ray entering a layer of higher sound velocity is bent away from the layer, while a ray entering a lower sound velocity layer is bent into the layer. Ray tracing can be either graphical or numerical for solving the problem of computing ray trajectories through a known spatial distribution of refractive indices. For this study, assume rays striking the bottom are reflected specularly. The velocity profile used in the HARPO model was a simplified version of the in-situ data measured on 12 June 1990. Seasonal variations of the sound velocity profile on the Nanoose Bay range measured over a year and the 12 June 1990 velocity profile are shown in Figure 2. Variational changes in water column parameters are discussed in detail by Helton [8]. Seasonal changes in wind, mountain river runoff and convective mixing caused abrupt changes in the velocity profiles.

Several assumptions are used to calculate the sound intensity along the ray path. The velocity changes linearly with depth (*ie.*, the water is horizontally stratified), and sound velocity at the operational depth does not vary more than 5 percent from the surface velocity. Therefore, those rays which leave the projector at a moderate angle don't get steep, and the sine of the angle can be approximated as the angle itself.

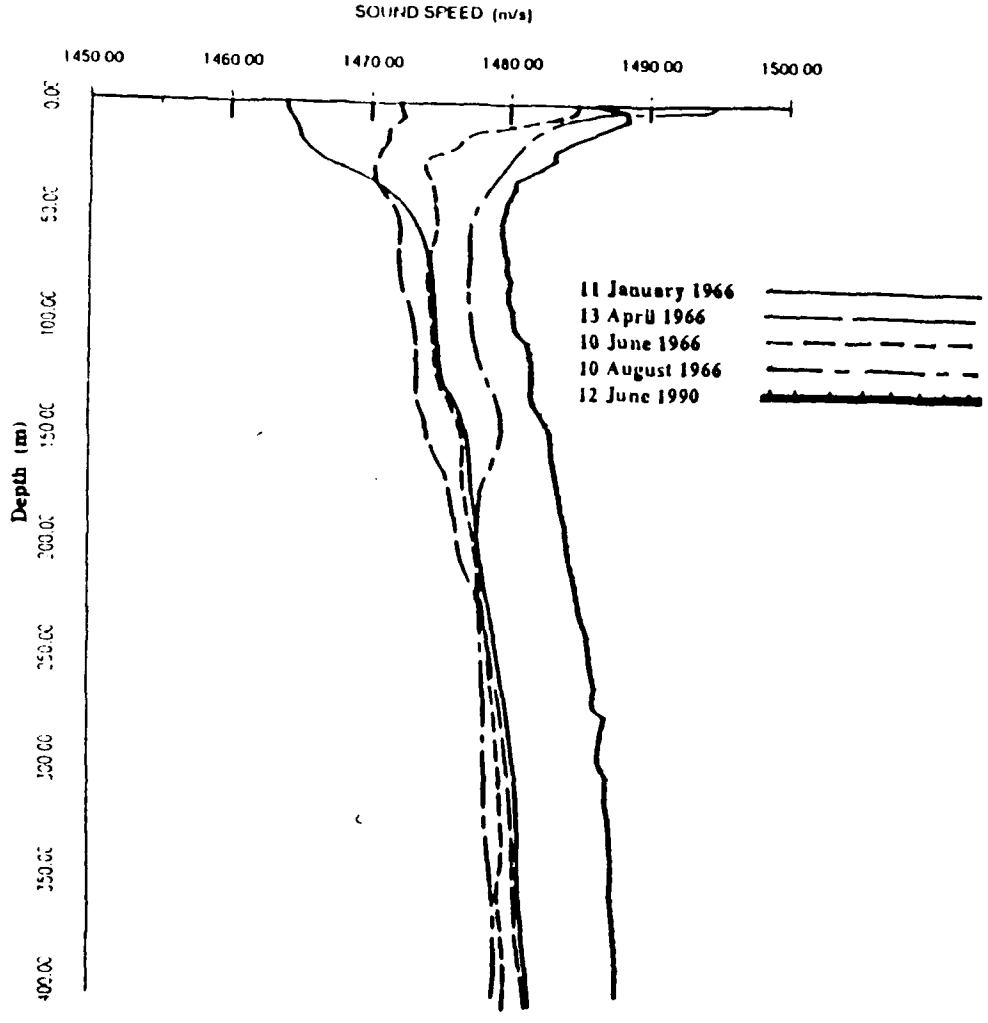

FIGURE 2. Typical Seasonal variations of the velocity profiles at the Nanoose Bay Range [9, Figure A.1. ; 10].

The transmission loss, TL, is given by

$$TL = 10 \log (SL/AL_{fop}) \qquad (3)$$

where

SL = source strength level, (intensity)

AL_{fop} = measured level at the face-of-phone, (intensity).

The transmission anomaly, A, is how the transmission loss differs from spherical spreading. It is generally defined as

$$A = 10 \log (SL/AL_{fop}*R^2), \quad (4)$$

where

SL/AL_{fop}, describes the spreading and is the ratio of the source level to the receive level at the face of hydrophone

and

R is the slant range.

The transmission loss along the ray path is directly proportional to the square of the path length if only the spherical spreading loss is taken into account. The intensity along a ray path changes when the sound wave reflects from the bottom or the surface boundary. The intensity also depends on the sound wavelength, the amount of energy focused, and how nearly perfect the focusing is. This is similar to the focusing of light by a lens. Sound has some travel time from the transducer to the location where the rays cross at the focal point (or caustic region). If the travel times are very different, pulsed tones would not interfere with each other and there would be no sound focused. The intensity at the focal location in a convergence zone is larger than the signal for a spherically spreading wave front at the same range. For this study, assume specular reflection (the ray hits the bottom at angle θ and reflects off at angle $-\theta$) and no reflection loss. Since the angle of incidence is equal to the angle of reflection, the reflected wave front has the same curvature and appears to come from an image source below the interface, similar to the Lloyd's mirror effect.

There is usually more than one propagation path between a source and receiver. Often one path will dominate, and its TL will be minimum compared to other paths.

Clay and Medwin [11] explain that when sound rays converge or diverge, the change of separation of closely spaced rays can be used to estimate the sound transmission loss. A caustic or focal point is the envelope of the family of rays when they converge. The geometry of two rays separated by a small amount but not converging is shown in Figure 3 [12]. The transmission loss between the source and receiver which are separated by a range R, can be deduced from the ray trace by determining the vertical separation of closely spaced rays, Δh.

The power radiated at the source within the angle $\Delta\theta$ of two closely spaced rays is, by definition, the same amount of power which radiates at the receiver within the same rays. The transmission loss from the source to the receiver is therefore

$$10 \log (I_1/I_2) = 10 \log (\Delta A_2/\Delta A_1) \quad (5)$$

where

I_1 is the intensity at the source

I_2 is the intensity at the receiver

ΔA_1 is the area in a one meter sphere

ΔA_2 is the area included by the ray pair at the receiver.

By substituting and applying Snell's Law equation (5) becomes

$$TL = 10 \log (R_h \, \Delta h/\Delta\theta \, \cos\theta_2/\cos\theta_1) = 10 \log (R_h \, \Delta h/\Delta\theta \, c_1/c_2) \quad (6)$$

where

R_h is the horizontal range from the source to the receiver (m)

Δh is the vertical separation (m)

$\Delta\theta$ is the initial angle between the two rays at the source (rad)

θ_1 is the angle from the horizontal at the source (rad)

θ_2 is the angle from the horizontal at the receiver (rad)

The bottom can be a relatively lossy medium, but if the receiver and transducer are close to the bottom, and if there is a fairly strong shallow water layer

or sound channel above them, the bottom can be expected to play a large role in the direction of the ray and amount of total transmission loss.

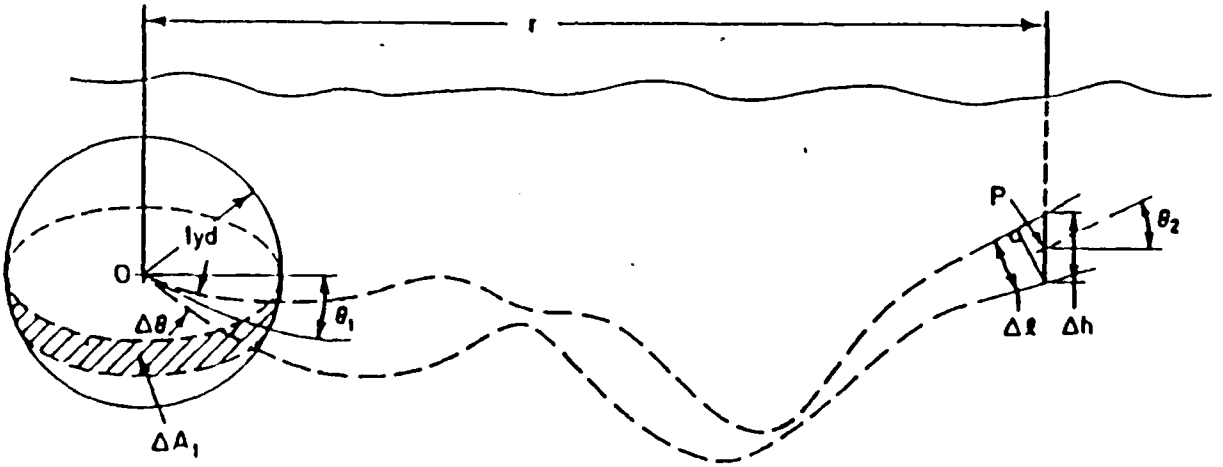

FIGURE 3. A diagram of the closely spaced rays used for transmission loss calculations [12, p.127].

Source level, SL, a function of frequency, is equal to the absolute level, AL, at the face-of-phone, fop, minus the transmission loss, TL, which is a function of range and frequency. The transmission loss is a combination of the spreading loss and frequency dependent absorptive losses, α, inherent in the medium over some range, R.

$$SL = AL_{fop} + TL \tag{7}$$

$$TL = S_{pr}L + \alpha R \tag{8}$$

Transmission loss is used to calculate the free-field sound pressure level, SPL. The Bolt, Beranek and Newman study of 1968 [9], suggested the transmission loss for Nanoose, TL_n, would be

$$TL_n = 19 \log R + 1 \text{ dB}, \quad 20<R<2000 \text{ yards} \tag{9}.$$

The equation currently used for the Nanoose range [13], takes into account the depths of the source and receiver. The equation is

$$S_{pr}L(R,Z) = 10\log(1/R^2 + 1/(R^2+4Z_sZ_r)) \quad (10)$$

where

$S_{pr}L$ is the spreading loss at slant range, R, and depth Z

Z_s is the depth of the source

Z_r is the depth of the receiver.

Derivation of equation (10) is given in Appendix B. This takes into account the addition of the signal along the surface path only. The pressure from the surface path component will add to the direct path component so the transmission loss will be less than that caused by purely spherical spreading. Bottom contour is not accounted for in either of these formulas.

The NUWES Underwater Noise Analysis Facility (UNAFAC) uses the following frequency dependent absorption formula based on the discussions of Clay and Medwin [11] and Urick [12]. The absorption formula is

$$\alpha_1 = (43.6*f^2 / (f^2 + 6400) + 2.55*10^{-4}*f^2) / 1000 \quad (11)$$

where

α_1 is the absorption coefficient, (dB/yd)

and

f is the acoustic frequency, (kHz)

The HARPO subroutine SLLOSS computes absorption using the Skretting-Leroy absorption formula [14] as

$$\alpha_2 = a* \omega^2/\omega_1^2 + b * \omega^2/(\omega_2^2 + \omega^2) \quad (12)$$

where

a is 0.006 dB/km

b is 0.2635 dB/km

ω_1 is 1000 Hz and ω_2 is 1700 Hz

α_2 is the absorption coefficient, (dB/km)

f is the acoustic frequency, (kHz).

The difference in the absorption values between equations (11) and (12) is shown in Table One. The loss values are close but do not agree and will not be compared in the qualitative analysis. The HARPO user may modify equation (12) by changing the values of ω_1 and ω_2 to find a closer fit, if quantitative absorption values are required. These absorption loss equations are valid for wavelengths much less than the depth of the water column. Other absorptive losses include attenuation, boundary zone, and refractive scattering losses. Attenuation is important at higher frequencies. Surface boundary zone losses are affected by wind, and refractive scattering loss can be caused by fine-scale changes in the sound speed profile. Only spreading loss will be addressed in this paper.

TABLE ONE

Frequency (kHz)	α NUWES (dB/m)	α SLLOSS (dB/m)	Difference (dB/m)
.1	$7.7 * 10^{-8}$	$9.688 * 10^{-7}$	$8.9 * 10^{-7}$
.2	$3.06 * 10^{-7}$	$3.838 * 10^{-6}$	$3.52 * 10^{-6}$
1	$7.7 * 10^{-6}$	$7.375 * 10^{-5}$	$6.61 * 10^{-5}$
2	$3.09 * 10^{-5}$	$1.77 * 10^{-4}$	$1.46 * 10^{-4}$
5	$1.9 * 10^{-4}$	$3.862 * 10^{-4}$	$1.96 * 10^{-4}$
10	$7.6 * 10^{-4}$	$8.563 * 10^{-4}$	$9.6 * 10^{-5}$

1.3.1 COHERENCE

Coherency is the degree to which the signal remains unchanged or undistorted by the process of transmission along some path, including reflection at the boundary. Whenever an omni-directional sound source is present, both surface

and bottom reflected waves may arrive at a given point to combine with the direct wave. Depending on their relative phase, these waves may either reinforce to produce greater pressure than the direct wave alone, or partially cancel to produce less pressure. Incoherence most often occurs with high frequencies, longer ranges, inhomogeneous water, and rough boundaries. If the surface is relatively smooth compared to wavelength, the reflected wave acts as if it were emitted by an image located a distance Z_T above or below the surface and 180^o out of phase with the source, where Z_T is the depth of the receiver. An incoherent wave has a random phase that is uniformly distributed over a length period of 2π; its mean power densities may be added. A coherent wave has a constant phase and a total power density, obtained by summing the individual fields vectorially to determine the power density from the resulting total field. For the Nanoose example, the pressure amplitudes should be added incoherently.

Scattering strength increases with increasing frequency and depends on bottom and subbottom composition and roughness. In Physics of Sound in the Sea [15], scattering strength is described in detail. As grazing angles tend to 0^o, scattering strength decreases rapidly to become negligible. If the bottom has irregular features such as rocks and boulders, one can expect a large amount of backscatter. Clay and Medwin [11] suggest that for a 1 kHz sonar signal, an irregularity as small as 1 meter is large enough to strongly scatter the sound. Although the surface boundary is considered to be where the primary effects of multipath interference originate, acoustics involving the bottom boundary is an important source of specular reflection, back scattering, absorption into, and transmission from bottom sediments. Exact solutions require completely specified geometry and reflection coefficients. The refraction and transmission of sound at the water/sediment boundary can be expressed in terms of the ratio of the acoustic impedances, $\rho_1 c_1/\rho_2 c_2$, and angle of incidence with the bottom. After incidence on

a rough boundary, the reflected signal will be reduced in amplitude and changed in phase by the reflection coefficient of that boundary. If the value of the speed of sound for the subbottom appears low, it may be due to a sloping profile giving a low apparent velocity.

The ocean bottom has both topography and reflectivity (material property such as porosity). Newhall *et. al.*, maintain that reflectivity, which is a function of the local geology, angle of ray incidence, and acoustic frequency can be described by the plane wave reflection coefficient [16]. Based on the grazing angle and knowing the composition of the bottom, the HARPO user would look up the reflection coefficient in a table. Bottom loss is usually measured by comparing direct path to bottom bounce path after subtracting spreading loss for path length differences. Bottom loss can be expressed as 20 log $\mathcal{R}$, where $\mathcal{R}$ is the reflection coefficient, and is small for small angles. The UNAFAC equations and HARPO do not incorporate the reflection coefficient at this time. More discussion is beyond the scope of this paper and readers are directed to Morris *et. al.*, who explain that some models take into account speed of compressional and shear waves in the sediment, absorption coefficients, density, and the thickness of the subbottom layers [17].

1.4 HARPO

1.4.1 OVERVIEW

In the past, various forms of the parabolic equation were considered the only way to handle change in bottom contour. Some models have become available that use ray tracing and take this into account. This section is a brief overview of the theory behind the HARPO model.

HARPO stands for the Hamiltonian Acoustic Ray-tracing Program for the Ocean. It is a general purpose FORTRAN ray tracing program which traces three-dimensional paths of acoustic rays through model oceans. It can be used to take into

account the 3 dimensionality of oceans and to compute reflections from complicated bottom models. HARPO calculates ray paths by numerically integrating Hamilton's equations in four dimensions, three spatial and one temporal, for earth-centered spherical-polar coordinates ρ,θ,ϕ and time t, as well as its first spatial and temporal derivatives. Jones *et. al.*, have shown [14] the solutions to the wave equation are related to paths that satisfy Fermat's principle, and that Hamilton's equations can be integrated to construct such paths. In Cartesian coordinates, Hamilton's equations take the form

$$dx_i/d\tau = \delta H/\delta k_i \ ; \ dk_i/d\tau = -\delta H/\delta x_i \ , \quad i = 1 \text{ to } 3 \qquad (13)$$

where

τ is sometimes time,but depends on how the Hamiltonian, H, is defined

k_i are wave number components

x_i are coordinates of a point on the ray path

To solve equation (13) for the ray path, the user chooses initial values for the quantities of x_i and k_i integrating results in six differential equations. For acoustic waves in the ocean, the Hamiltonian, constant along a ray path, is defined as

$$H(x_i,k_i) = (\omega - k * V(x_i))^2 - C^2(x_i)k^2 = 0 \qquad (14)$$

where

$V(x_i)$ is the ocean current, may be time dependent

$C(x_i)$ is the sound speed field, may be time dependent

and

ω is the angular wave frequency.

Equation (14) shows that the effect of a three dimensional vector-current field is included in the definition of the Hamiltonian Hamilton's equations are equivalent to the Eikonal equation for determining the ray path.

Hamiltonian ray tracing is an alternative to segmented methods and requires the ocean to be modeled as a continuous three-dimensional function with continuous

gradients. Each ray path is computed by numerically integrating Hamilton's equations with a different set of initial conditions. Because it uses continuous models, this method avoids false caustics and discontinuous ray paths. These properties are encountered in conventional ray tracing methods, which use layers where each acoustic ray path segment is computed alone. The reader is directed to Jones, Riley and Georges [14], who have documented the software. The user defines an ocean model with a unique velocity profile and bottom depth.

A version of HARPO has recently been developed by Georges *et. al.* [18] to run on a personal computer (PC) using a FORTRAN compiler as an improvement to the Digital Equipment Corporation, VAX version. The HARPO model will give the user freedom to manipulate the various parameters which affect the sound propagation, including bottom contour, current and wind influence. It can display ray traces both graphically and in tabular form.

HARPO can describe the geometry of the ray path, calculate a pulse travel time and phase time, and compute the Doppler shift, rate of change of phase (if the user has chosen the ocean to vary in time), absorption and geometric path length. It allows continuous three-dimensional models of the refractive-index field and two-dimensional models of reflecting surfaces. The user may trade computing speed for accuracy by specifying the maximum allowable integration error per step. I have only manipulated the bottom topography by introducing a Lorentzian shaped ridge to the flat bottom model.

1.4.2 LIMITATIONS AND ASSUMPTIONS

Criteria for using ray tracing include making sure there is a fractional change in gradient, g, over a wavelength, λ, which is small compared to sound speed, c, (ie., $g\lambda << c$) where $g = dc/dz = (c_1-c_2)/(Z_1-Z_2)$, therefore ray models are more accurate at higher frequencies (*e.g.*, above 1 kHz). A second criterion states that the radius of

curvature is much greater than the wavelength. This means that only plane waves in the far field are acceptable. The velocity is assumed to change linearly with depth. Because it is based on ray theory, HARPO has the same limitations. The ocean model the user inserts must be deterministic, not random. It accepts only bottom models with continuous surface, slope and curvature. For example, wedge shaped surfaces are not allowed. It cannot handle refraction at discontinuities of refractive indices or its gradients.

HARPO does not check to be sure the input from the user is reasonable, nor does it apply corrections for diffraction or partial reflections. It does not check to see if ocean models satisfy physical conservation laws and boundary conditions. It does not check any models to see if they satisfy continuity, or physical boundary conditions, nor does it automatically compute amplitude or transmission loss. Therefore, the total amplitude at a receiver must be computed by the user by combining the absorption, reflection losses and focusing listed for each ray. The user must also decide whether to add the contributions of multipath rays coherently or incoherently.

HARPO assumes conservation of energy within the bundle of rays, so the wave intensity is inversely proportional to the cross sectional area called a flux tube. When that area becomes zero, ray theory predicts infinite energy density (a caustic, where two or more rays cross).

CHAPTER 2

ANALYSIS

2.1 HARPO SETUP

While modeling the ray paths, the frequency and angle of incidence were held constant. The difficulty with the topography was interpolating the data from bathymetry charts into a form usable to the code without taking up too much storage space and thus increasing the program run time. The rays of the most interest are the eigenrays connecting the source to the receiver. That is the direct path, the one surface bounce, the one bottom bounce and the one bottom/surface bounce. "Shooting techniques" must be used to find these rays. The user sends out a fan of rays at different launch angles which bracket the receiver range, depth and azimuth. These ray launch angles are then linearly interpolated, new rays are launched based on this first guess. This procedure is iterated until a given ray has come within a specified distance of the receiver. The user gets an accurate first guess for the launch angles to other ranges (elements) by finding the eigenray for the farthest range (element) radially. I was not able to establish the appropriate eigenrays to determine the actual transmission loss levels, this results in a strictly qualitative analysis.

The GLORENZ subroutine superimposes a Lorentzian shaped ridge on a spherical surface of any height and width to represent the steep slope and hills typical on the Nanoose Bay range. The west end of the Nanoose Bay range was the incentive for the steep slope representation. The bathymetric profile of the Nanoose Bay range along the centerline is shown in Figure 4. The hilly bottom contour profile across Array 7 is shown in Figure 5. These are models of the most commonly occurring bottom type, beside the flat bottom, on the Nanoose range shown in Figure 1.

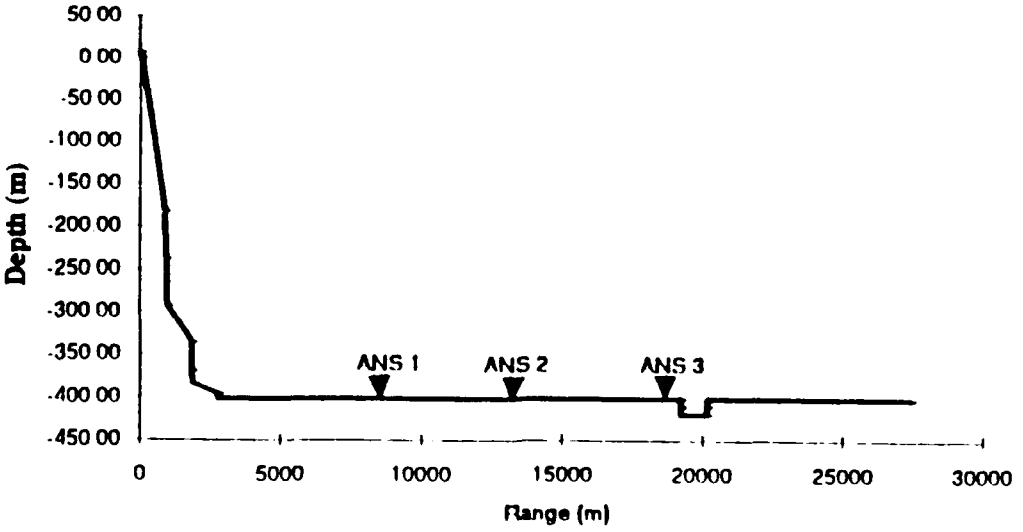

FIGURE 4. The Bathymetric profile of the Nanoose Bay range along the centerline.

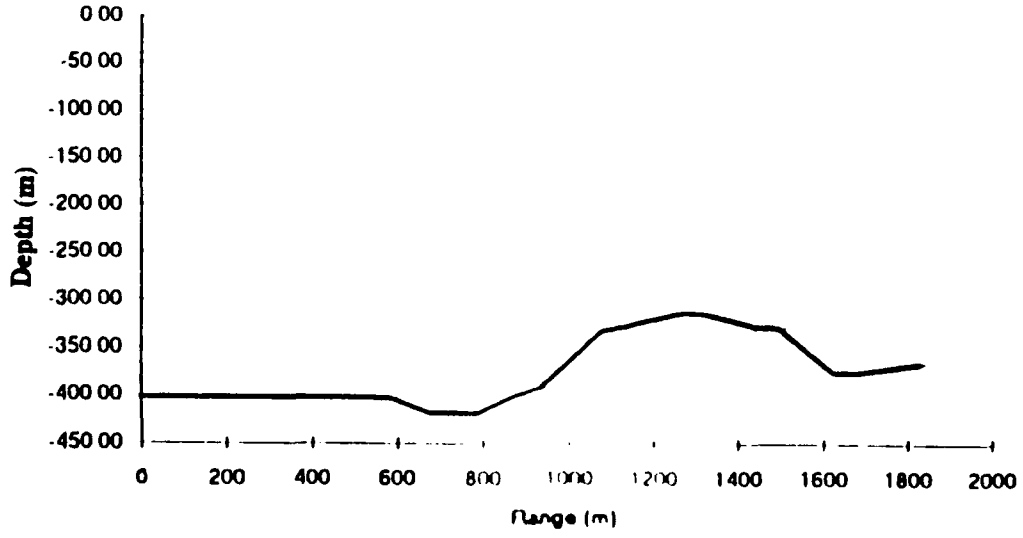

FIGURE 5. The bathymetric profile across array 7 on the Nanoose Bay range.

Georges points out "the bathymetry sensitivity is critical to raypath stability issues, which affect signal processing, and topography" [18, p. 203]. There are

many rays both upward and downward from the horizontal, for clarity only -2 degree through -6 degree launch angles have been shown in Figures 6 through 8 and 10.

2.2 HILL CONTOUR

The Lorentzian shaped hill topographies were put into the HARPO model at both 100m and 200m high as shown in the ray trace Figures 6 and 7. The larger hill is similar to the contour found on the Nanoose range in array 7 , as is shown in Figure 5. For modeling purposes, the area in front and behind the hill is flat. Compare the ray trace of the flat bottom in Figure 8 with that of the larger hill, Figure 7. The rays become steeper as they hit the hill. A shadow zone develops beyond and behind the hill. The angle dependent bottom reflection coefficient increases when the grazing angle increases. The steeper rays increase the reflection coefficient and increase the bottom loss experienced by the sound. The ray paths are warped, the path lengths are different, and spreading loss is increased. The channel trapped ray is destroyed.

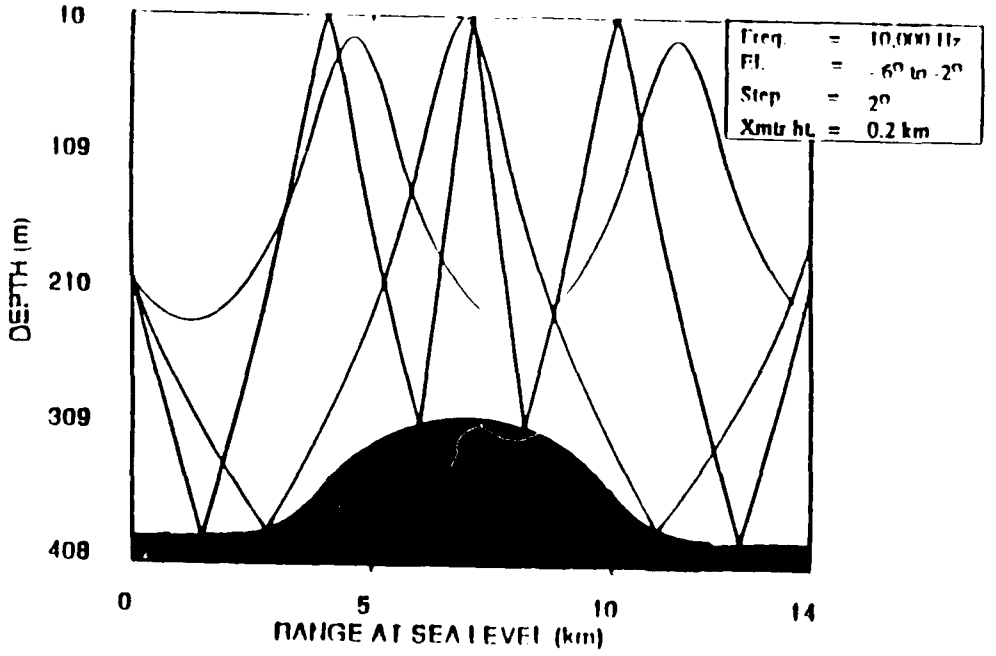

FIGURE 6. A HARPO ray trace with small hill topography.

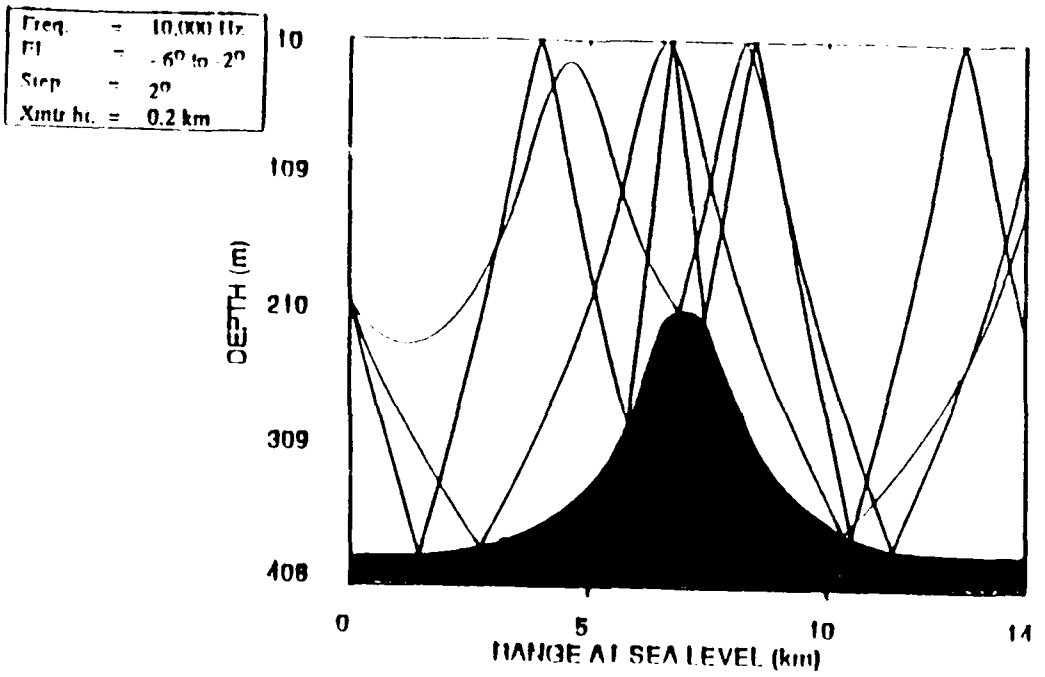

FIGURE 7. A HARPO ray trace with large hill topography.

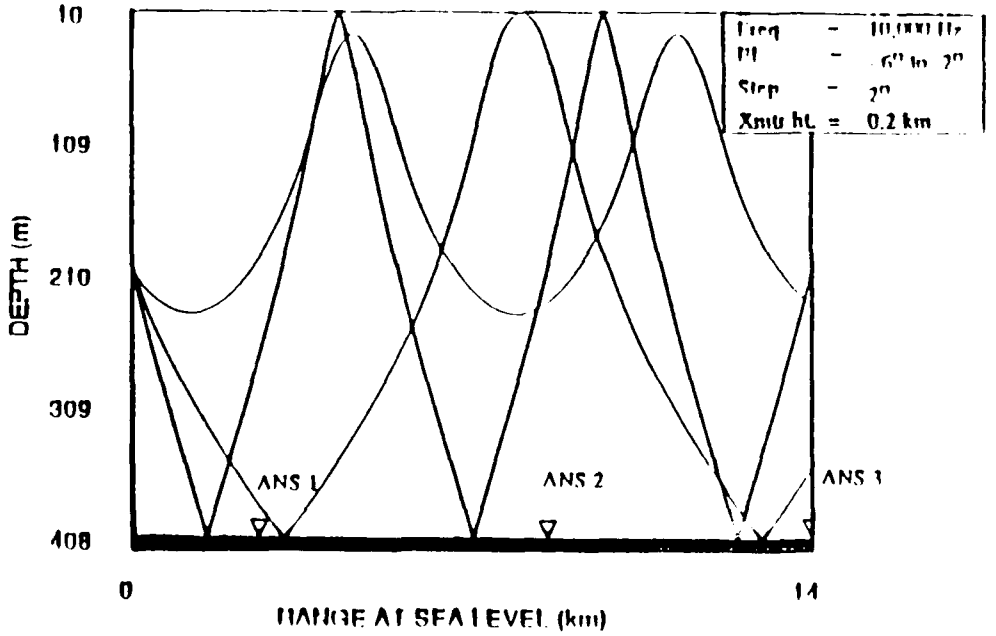

FIGURE 8. A HARPO ray trace with flat topography.

The smaller hill does not effect the ray as much as the larger hill since it is below the sound channel. The channel trapped ray is undisturbed. The ray bottom interaction is dependent on the height of the hill with respect to the depth of the transducer and the shape of the velocity profile. Rays leaving the source at steep angles interact with the hill and suffer reflection loss. This phenomena has been studied by Jensen, who wrote, "Ray angles steepen by twice the bottom slope per bounce, *ie*. around 28^{o} and hence can undergo a maximum of three upslope reflections before being redirected back toward the source"[19, p. 193]. The example in Figure 9 shows the near-grazing rays get over the top and get trapped in the upper sound layer. In front of the hill, the propagation is dominated by steep bottom bounce paths. Part of the sound bounces back toward the source to create a large caustic or focal region. Volume reverberation increases, causing a low signal-to-noise ratio due to the rays bouncing off the slope. The volume of water in front of it is ensonified.

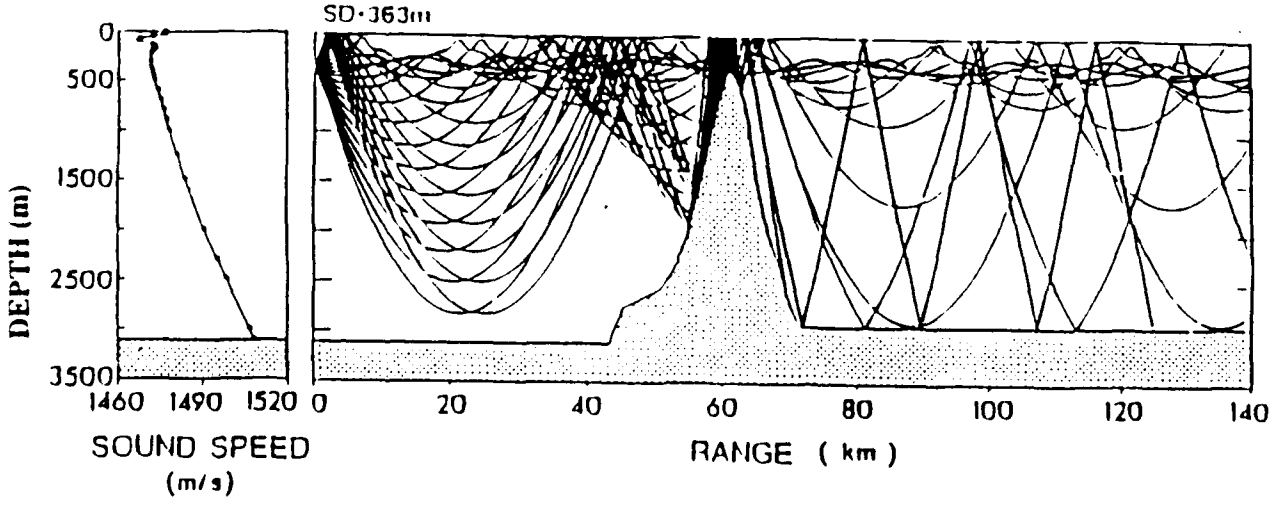

FIGURE 9. A ray trace of the sound propagation across a seamount [18, p. 193].

Multiphone averaging used to reduce the multipath effect will not be enough to reconcile the signal, in the case of the larger hill. Based on the fact that the bottom is very lossy, I would expect the sound in the flat contour to die out more quickly. The rays in the hill and slope examples tended to get trapped in the sound channel. In the flat example, the rays just bend and don't hit the bottom, but in the hill example, the rays are distorted. The minus two degree ray, for example, would not hit the bottom with the slope, whereas on the hill it does. Then the sound will experience more loss due to the lossy bottom.

2.3 SLOPE CONTOUR

The slope topography used in the HARPO model is similar to the western slope on the centerline of the Nanoose Bay range. The bottom contour of the range along the centerline is shown in Figure 4. The centerline of the range is where most of the events tested on range take place. Compare the flat contour ray trace in Figure 8 to the slope topography ray trace, Figure 10. The sound is focused back toward the source and the volume of water in front of the slope is ensonified. This is similar to the effect of the hill but more pronounced. The rays angles are steepened, and the sound has become focused.

Three Ambient Noise Source (ANS) hydrophones (ANS 1, ANS 2, and ANS 3) are permanently mounted approximately 12 feet from the floor of the Nanoose range as shown in Figures 4 and 8. Local roughness will cause scattering because of their close proximity to the ocean floor . ANS 1 is nearest the base of the steep slope and may be influenced by the increased reverberation, as the volume of water in front of the slope is ensonified. This may cause a low signal to noise ratio. As the autogain of ANS 1 increases to compensate for the reverberation, the hydrophone may not detect signals or radiating noise. ANS 2 and ANS 3 are further from the steep slope and will have a higher signal-to-noise ratio. In the flat bottom

contour example, sound ray paths are considerably more influenced by the velocity profile than the irregular bottom contour examples.

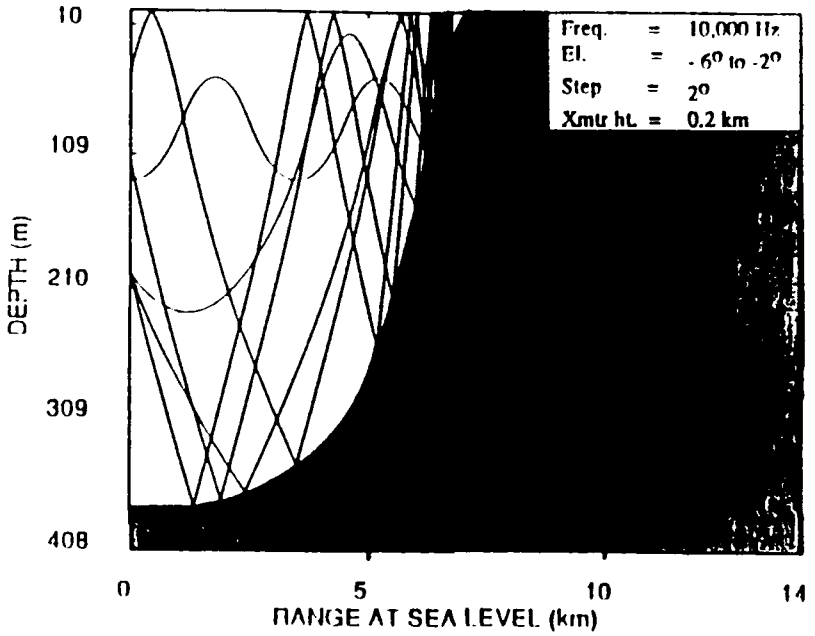

FIGURE 10. HARPO ray trace with steep slope topography.

CHAPTER 3

TRANSMISSION LOSS MEASUREMENTS USING ANS

3.1 MEASUREMENT SETUP

The objective of the test performed at the Nanoose Bay range on 12 June 1990 was to calibrate the three ANS hydrophones. These hydrophones were evenly spaced along the bottom of the range over a relatively flat contour. It was hoped that these results could also be used as the baseline set of measurements of spatially separated receivers over a flat bottom contour. This baseline can be compared with future in-situ measurements with the same receiver spacing over an irregular bottom contour to quantitatively determine the difference in transmission loss between the flat and irregular bottom contours. The Sonar Acoustic Target Source (SATS) transducer array [20] was used to project tones during the test. SATS is a TR-292/WQM-6. SATS is a target source and measuring system used for the certification of sonar systems. It is semi-portable, surface deployed over the side equipment. It is made of several components, two of which were required to span the desired frequencies. A random sample of center frequencies of 100, 200, 500, 1 kHz, 2 kHz, 5 kHz, 10 kHz, and 20 kHz were projected from SATS. The channel 4 projector, TR-295/WQM-6, consisted of a coated ceramic sphere mounted on a base plate through which a cable and penetrator housing entered. For the lower frequencies, projector TR-294/WQM-6 was used. It was composed of six bender bar assemblies surrounded by a oil-filled neoprene boot, a compliant tube assembly surrounded by a rubber boot, shields and guard bars, a transformer, and cover and frame assemblies. The hydrophones used to acquire the sound were three ITC-H68A hydrophones. These phones were on 12 foot frames planted on the bottom of

the Nanoose Bay, approximately 6,000 meters from each other as shown in Figures 1 and 8.

During the test, SATS projected a series of continuous wave signals from a location between ANS 2 and ANS 3 at a depth of approximate 250 feet.

3.2 ANALYSIS OF RESULTS

At least 10.5 seconds was required for a sound wavefront to get from SATS to the slope and back to ANS 1. The analysis was averaged over a 4 to 23 second time period during the 25 to 55 second broadcast. One would expect the level at ANS 1 to be different than the other ANS hydrophones if the slope interfered with the direct path.

Table Two contains source level estimates of the data at the ANS hydrophones. This is the absolute level at the face-of-phone minus the Nanoose transmission loss (equation 10). There were no low frequency results due to the surrounding high ambient conditions caused by several craft generators. The SNR was not high enough to give me confidence in the output level at the low frequencies. There were no significant differences in the levels of the three hydrophones over the relatively flat bottom. The level of reverberation was too low to interfere with the direct path. This may have been due to the fact that the bottom and slope are covered with mud and ooze, creating a very lossy bottom. No shadowing occurred because the area between the three phones was relatively flat.

TABLE TWO

Freq. (kHz)	PAMS SL_{real} (dB)	ANS 1 SL (dB)	ANS 2 SL (dB)	ANS 3 SL (dB)
2	162	156	154	162
5	159	162	157	161
10	164	163	161	162
20	164	163	161	162

3.3 RECOMMENDATIONS FOR THE NEXT EXPERIMENT

To measure the effects of an irregular bottom contour, an additional set of tests should include setting one of the receivers on the opposite side of the hill from the transducer, where the expected signal level will be much lower. Next, position the receivers along the base of the steep slope, and place a directive source beyond it. The directive source could then be aimed in several directions to measure the effect of the volume reverberation and focusing off the slope. Another good test scenario would be to position an omni-directional source far from the slope with a directive receiver located near the slope.

CHAPTER 4

CONCLUSIONS AND RECOMMENDATIONS

This study focuses on ray trace deformation due to changing bottom contours. The HARPO program was manipulated to model several bottom contour types, but actual transmission loss levels were not obtained. This results in a strictly qualitative analysis.

Changes in bottom contour have been shown to affect sound propagation parameters, such as changes in path length and angle of incidence. The result is a difference between the predicted focal point (caustic) locations for flat contour and the irregular contour. The results of in-situ measurements are valuable as a quantitative baseline, and can be compared to future transmission loss level measurements acquired from receivers at the same range separation over irregular bottom boundaries.

Other variables can be introduced to the HARPO model, including ocean currents, which can be used to predict the influence of the tidal currents prevalent in this region. The reflection coefficient for the bottom should be added to the program capability.

On the Nanoose Bay range, a directive beam in the westward direction would simulate the steep slope model, while the hill portrayed is a simulation of the contour encountered in array 7. Other test ranges can be modeled in this same manner. The Dabob range is much smaller but has similar steep boundaries. The Quinault Underwater Tracking Range is relatively flat and very shallow.

Quantitative transmission loss data will be useful in further studies of ray tracing, and would be a valuable addition to the studies already accomplished on the NUWES underwater tracking ranges.

REFERENCES

1. Staal, P.R.and Desharnais, F., Propagation-Loss Measurements and Modelling for Topographically Smooth and Rough Seabeds; Report no DREA/TM-89/214, Defense Research Establishment Atlantic, Dartmouth (Nova Scotia), June 1989.

2. Keys, M. NUWES Underwater Acoustic Measurement and Analysis: An Overview December 1990.

3. NUWES Drawing No. 22261

4. Middleton, W.A.,1973, Physical Oceanographic Characteristics of the Nanoose Range, Naval Torpedo Station Report NAVTORPSTA 1163,Keyport, WA, p.113.

5. Herlinveaux, R.H. , and Garrison, G.R., Appraisal of the Proposed Underwater Tracking Range in the Strait of Georgia, 1962, Pacific Oceanographic Group, Fisheries Research Board of Canada, Nanaimo, B.C.

6. Kinsler, L.E., Frey, A. R., Coppens, A.B., and Sanders, J.A., Fundamentals of Acoustics, pp. 461-162, third ed., New York: Wiley-Interscience, 1982.

7. McCammon, D. F., "Underwater Propagation", ACS 511 unpublished course notes, The Pennsylvania State University, June 1988.

8. Helton, R. A., Deep Water Range Acoustic Transmission Model and Transmission Distance Estimates,pp. ii, 139, NUWES, Applied Research Technical Note 84-3 of April 1984.

9. Bolt, Beranek and Newman, Inc., Private communication, 1968.

10. Unger, S., Unpublished measurements taken on the Nanoose Bay range, 12 June 1991.

11. Clay, C.S. and Medwin, H., Acoustic Oceanography: Principles and Applications, John Wiley and Sons, New York, 1988, pp.83-106 ,358-387.

12. Urick, R.J., Principles of Underwater Sound, third ed., New York: McGraw-Hill, 1983, pp. 105-109, 126-128.

REFERENCES cont.

13. UNAFAC Source Code, Math library "math_lic.c",NUWES Acoustics Division, 1990.

14. Jones, R.M., Riley, J.P. and Georges, T.M, HARPO A Versatile Three Dimensional Hamiltonian Ray-Tracing Program for Acoustic Waves in an Ocean with Irregular Bottom, Wave Propagation Laboratory, Boulder, Colorado, October 1986.

15. Physics of Sound in the Sea originally issued as Summary Technical Report of Division 6, NDRC, Volume 8, Washington D.C. 1946 pp.41-59.

16. Newhall, A. E. and Lynch, J. F. Chiu, C.S. and Daugherty, J.R.,Improvements in Three-Dimensional Ray tracing codes for Underwater Acoustics submitted to IMACS, April 89.

17. Morris, H.E., Hamilton,E.L.,Bucker, H.P., and Bachman, R.T., Interaction of Sound with the Ocean Bottom: A Three-year Summary: NOSC Technical Report 242, pp.1-77, 30 April 78.

18. Georges T. M., Jones, R. M. and Lawrence, R. S. A PC VERSION OF THE *HARPO* OCEAN ACOUSTIC RAY-TRACING PROGRAM, NOAA Technical Memorandum ERL WPL-180, Wave Propagation Laboratory, Boulder Colorado, June 1990.

19. Jensen, F.B., "Wave theory Modeling: A Convenient Approach to CW and Pulse Propagation Modeling in Low-Frequency Acoustics", IEEE *Journal of Oceanic Engineering*, **13**(4), 186-197, 1988.

20. NAVSHIPS 0967-489-9930, Operator's Manual AN/WQM-6 Test Set Sonar, Rev. C, 30 September 1980.

APPENDIX A

REFERENCES FOR ALTERNATE MODELS AVAILABLE

1. Medeiros, R.C., RAYMODE Passive Propagation Loss Program Performance Specification, New England Technical Services (NETS), Doc. No. 8205 1982, revised 7/01/83.

2. Weinberg, H., Generic Sonar Model, NUSC Technical Document 5971D, NUSC Newport RI 1985.

3. Schmidt,H., SAFARI, Seismo-Acoustic Fast-field Algorithm for Range Independent Environments, User's Guide Report SR-113, SACLANT Undersea Research Center, San Bartolomeo Italy, 1988.

4. Goddard,R.P., REVGEN-4, High Fidelity Simulation of Sonar Pulses, APL-UW 8505, APL, UW, Seattle, Wa,1986.

5. PC FACT generates Transmission loss data. It is a ray model for range independent (single speed profile, flat bottom) environments. Useful over 10-3500 Hz.

6. Weinberg,H., "Application of Ray Theory to acoustic propagation in horizontally stratified oceans.", *J. Acoust. Soc. Am.*, **58**(1) 97-110, 1975.

7. Schmidt, H., and Jensen, F.B.,"Efficient Numerical Solution Technique for Wave Propagation in Horizontally Stratified Ocean Environments" Report SM-173 SACLANT ASW Research Center, La Spezia, Italy, 1984.

APPENDIX B

NANOOSE TRANSMISSION LOSS DERIVATION

The Nanoose range site transmission loss equation was developed based on geometry of a surface bounce adding with the direct path [20] shown in Figure 11. The surface-bounce path range, R_S is

$$R_S = L_1 + L_2 = (R_h^2 + (Z_S + Z_T)^2)^{1/2} \quad \text{(A1)}.$$

where R_h, the horizontal range is

$$R_h = (R^2 + (Z_S - Z_T)^2)^{1/2} \quad \text{(A2)},$$

Then

$$\begin{aligned} R_S &= (R^2 - (Z_S - Z_T)^2 + (Z_S + Z_T)^2)^{1/2} \\ &= (R^2 - Z_S^2 + 2Z_SZ_T - Z_T^2 + Z_S^2 + 2Z_SZ_T + Z_T^2)^{1/2} \\ &= (R^2 + 4Z_SZ_T)^{1/2} \end{aligned} \quad \text{(A3)}$$

Assume only the first order surface and the direct signals come in to the receiver.

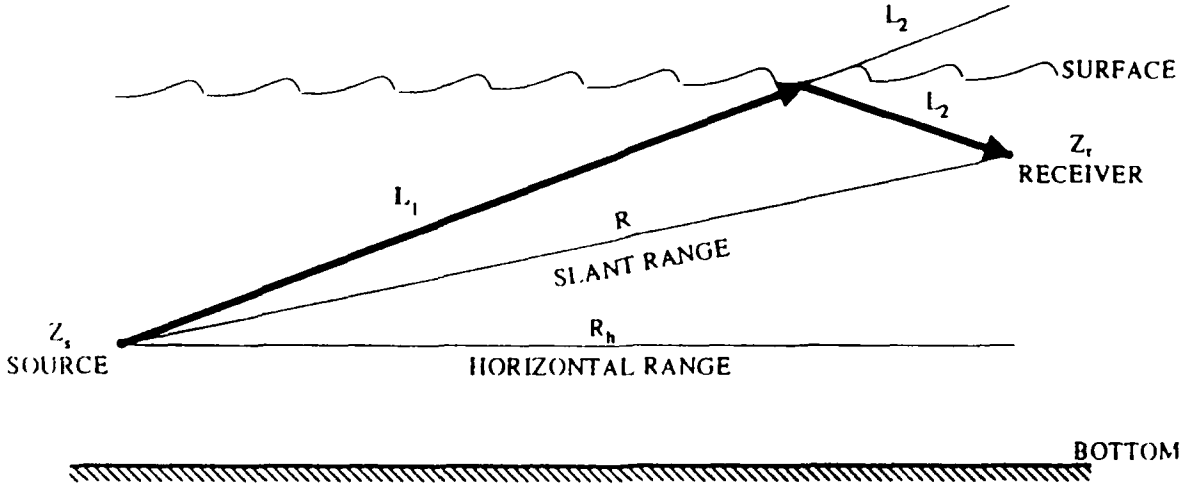

FIGURE 11. A Nanoose transmission loss diagram.

The received signal, r(t), then becomes

$$r(t) = s(t)/R^2 + s(t)/R_s^2 \qquad \text{(A4)},$$

where

s(t) is the source signal

r(t) is the received signal.

Assuming the surface is a perfect reflector,

$$r(t) = s(t)\,(1/R^2 + 1/(R^2 + 4Z_sZ_r)) \qquad \text{(A5)}.$$

The spreading loss becomes

$$S_{pr}L(R,Z) = 10\log(1/R^2 + 1/(R^2+4Z_sZ_r)) \qquad \text{(A6)}$$

where

SprL is the spreading loss at slant range, R, and depth Z

Z_s is the depth of the source

Z_r is the depth of the receiver.

Given the transmission loss is the spreading loss pluss the absorption loss,

$$TL = S_{pr}L + \alpha R$$

the Nanoose transmission loss equation, TL_N, becomes:

$$TL_N = 10\log(1/R^2 + 1/(R^2 + 4Z_sZ_r)) + \alpha R. \qquad \text{(A7)}$$

The B,B & N study of 1968 [9] suggested the transmission loss for Nanoose, TL_n, would be

$$TL_n = 19\log R + 1\text{ dB} + \alpha R\ ,\ 20<R<2000\text{ yards} \qquad \text{(A8)}$$

The difference between the two equations begins to get measurable at long distances. For example,

Given:

R= 1900 yds

$Z_s = Z_r = 200$ feet

$\alpha = 8.563 * 10\text{-}4$ dB/yd

$TL_N = 67.2$ dB and $TL_n = 64.9$ dB, therefore $\Delta TL = 2.3$